RSC Advances

Preparation of cubane -1, 4-dicarboxylate-Zn-Al layered double hydroxide nanohybrid: Comparison of structural and optical properties between experimental and calculated results

Journal:	*RSC Advances*
Manuscript ID:	RA-ART-05-2015-009716.R1
Article Type:	Paper
Date Submitted by the Author:	18-Jul-2015
Complete List of Authors:	Rezvani, Zolfaghar; Azarbaijan Shahid Madani University, Chemistry Arjomandi Rad, Farzad; Azarbaijan Shahid Madani University, Chemistry Khodam, Fatemeh; Azarbaijan Shahid Madani University, Chemistry

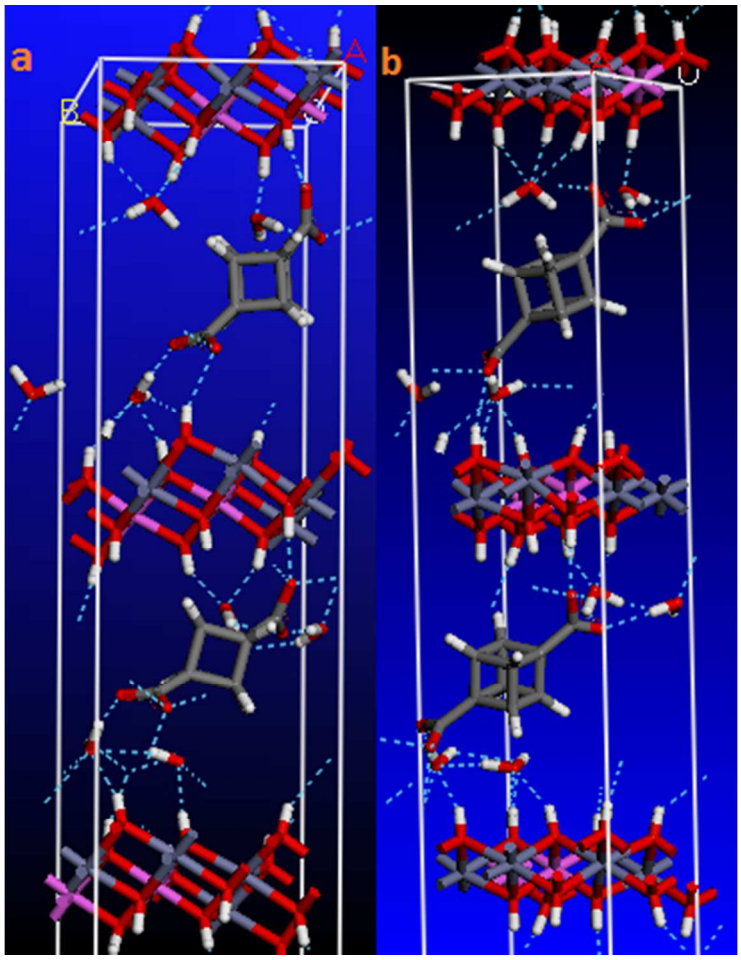

Graphical abstract
77x100mm (120 x 120 DPI)

RSC Advances

ARTICLE

Preparation of cubane -1, 4-dicarboxylate-Zn-Al layered double hydroxide nanohybrid: Comparison of structural and optical properties between experimental and calculated results

Received 00th January 20xx,
Accepted 00th January 20xx

DOI: 10.1039/x0xx00000x

www.rsc.org/

Zolfaghar Rezvani*, Farzad Arjomandi Rad and Fatemeh Khodam

In the present research, we report cubane-1,4-dicarboxylate anions(cuban-dc) assembled into Zn_2Al layered double hydroxide (LDH) inorganic host using coprecipitation method, in which solutions of Zn (II) and Al (III) nitrate salts react with an alkaline solution of cubane-1,4-dicarboxylic acid . Powder x-ray diffraction, FTIR spectroscopy, elemental analyses, and thermal gravimetric analysis (TGA) were used to characterize successful incorporation of the cubane-1, 4-dicarboxylate anions into the interlayer space of LDH. Periodic density functional theory was employed to understand the structural and electronic properties of the cubane-dc-Zn_2Al-LDH system. Quantum mechanics study was supported by periodic density functional theory (DFT) calculation which predicts appropriate values for structural and optical properties of cubane-dc-Zn_2Al-LDH. Optical and structural theoretical results are in good agreement with the experimental results, which shows that when cubane-1, 4-dicarboxylate anions intercalate in Zn-Al-LDH, they cause red shift and subsequently decrease of band gap energy in comparison with LDHs that contain small anions.

1. Introduction

Hydrotalcite, known as layered double hydroxides (LDHs), forms a significant class of readily synthesized clay-like nanoscale minerals [1,2]. Layered double hydroxides (LDHs) are a class of anionic clays whose structure can be described as containing brucite $[Mg(OH)_2]$-like layers in which some of the divalent cations have been replaced by trivalent ions, giving positively charged sheets.[3] This charge is balanced with intercalation of anions in the hydrated interlayer areas. These structures can be represented using the following general formula: $[M^{2+}_{1-x}M^{3+}_{x}(OH)_2]^{x+}[(A^{n-})_{x/n}.mH_2O]$ where M^{2+} and M^{3+} are di- and trivalent metal cations respectively, and A^{n-} represents an exchangeable interlayer anion with the charge of n^-.[4]

LDH systems were widely studied from a molecular simulations point of view for promoting their potential applications.[5] Many organic anions including carboxylates, sulfonates, benzoates, and organic dye and biomolecular anions such as aminoacides ,enzymes, and drugs can be intercalated within the interlayers of LDHs.[6] These new materials can be used as delivery carriers for drug delivery, gene therapy applications, photochemical cells, and catalysis and also show potential photocatalytic properties with good optical behaviors.[7]

Recently, investigations of the LDHs-layers and interlayer-anion interactions have attracted more attention for developing new types of organic-inorganic hybrid photofuntional materials.[5] These investigations have been carried out by analyzing the geometric parameters, charge population, energy, atomic orbital populations, DOS (density of state), and PDOS (partial density of state) [8,9]using density functional theory.

Ni et al[8] reported the investigation of microscopic structures and electronic properties of LDHs containing F^-, Cl^-, Br^-, I^-, NO_3^-, IO_3^-,and ClO_4^- using density functional theory.

Yan et al reported[9] 9-fluorenone-2, 7-dicarboxylate (FDC) assembled into the Mg-Al- and Zn-Al-layered double hydroxide (LDH) systems and their solid-state photophysical properties. Based on their results, FDC/LDH has a lower band gap than pristine LDH. Also Yan et al reported combining experimental and theoretical studies on the luminescent properties of MOF system which gives a rapid way to prepare a highly ordered inorganic–organic hybrid system with improved fluorescence properties, and a deep understanding of the electronic structure of the 2D pillared polarized fluorescence materials.[10]

Lu et al applied periodic density functional theory for calculations the band energy of a ultrathin films (UTFs) based on sulfonated polythiophene/LDH system for investigation of luminescent properties.[11] Also Lu et al have reported uniform near-infrared (NIR) absorption and photoluminescence properties of Scy/LDH UTFs and molecular dynamic (MD) simulation calculations for understanding the order degree of Scy anions in a confined

[a] Department of Chemistry, Faculty of Basic Sciences, Azarbaijan Shahid Madani University, Tabriz, Iran, Fax: +98 413 432 7541; Tel: +98 413 432 7541; E-mail: zrezvani@azaruniv.ac.ir

Electronic Supplementary Information (ESI) available: [details of any supplementary information available should be included here]. See DOI: 10.1039/x0xx00000x

environment of LDH, as an important parameter in the polarized fluorescence property .[12]

The main researches on computational simulation of hydrotalcite-like compounds were carried out with classical molecular dynamics (MD) [13-15], which has been used in the structural investigation and dynamic simulation of the interlayer species.[16,17] In this simulation, force fields are often parameterized based on experimental data or electronic structure calculations. For previously mentioned reasons, the experimental information of the structure is limited and does not include the analysis of the wide variety of substitutions. DFT quantum calculations using periodic boundary conditions have reached sufficient accuracy to predict crystallographic and electronic properties of these minerals. However, the large unit cells of LDH make these calculations very expensive.[18]

For instance, the spatial distribution of DOS of LDHs and band structure analysis are used to explain the different catalytic activities of LDH nanocomposites.[19,20]

Molecular simulation calculations and its comparison with the experimental results is supported by periodic density functional theory (DFT) which predicts suitable assessments in the band structure energies and also optical capability of LDHs. Total electronic densities of states (TDOS) and partial electronic densities of states (PDOS) analyses expose perfect description of the band gap calculation. [21] The band gap energy of LDHs is found to depend on both layer composition and intercalated anions distribution. The absorption, which corresponds to the electron excitation from the valence to the conduction band, can be used to determine the nature and value of the optical band gap. [7]

Most reported DFT studies involved small inorganic anions in the LDH galleries, and very few reports focused on functional anionic species intercalated into LDH systems. [22] Chai et al [23] have shown that the electronic transition of Zn_2Al–NO_3-LDH is a direct process from oxygen atoms to metal atoms of the layer. Zn_2Al–NO_3-LDH has two strong UV absorption peaks at 230 and 300 nm, which is ascribed to the presence of nitrate anions in the interlayer space [24], according to which the second peak of Zn_2Al–NO_3-LDH (Eg_2=3.829± 0.032) can also be ascribed to the NO_3^- radicals of LDH.[7]

The main goal of this research is investigating the effect of cubane-1,4-dicarboxylate intercalation as a large organic anion on the electronic structure and band gap energy of the cubane-dc-Zn_2Al–LDH nanohybrid. Cubane derivatives are widely used as novel organic anions for high-energy explosives,[25] oligomeric compound and pharmaceutical materials.Cubane-1,4-dicarboxylic acid is straightforward piece of organic anion with two carboxylic head groups and rigid structure which case this anion be stable to the water molecules in the spatial environment of Zn_2Al –LDH.[26] In viewpoint of first classical geometry optimization, cubane-1,4 dicarboxylate anion has a symmetrical structure and unique position for bonding and nonbonding interaction with layer of LDHs.

In our previous work, we prepared Mg–Al hydrotalcite intercalated by cubane-dc anions and then studied the distribution of the cubane-dc anions at the molecular level by the molecular dynamic (MD) study. The aforementioned distribution resulted from non-bonding and the host–guest interactions based on van der Waals and electrostatic forces in cubane-dc-Mg-Al-LDH.[26]

In the present work the preparation of the Zn–Al hydrotalcite intercalated with the cubane-1,4-dicarboxylate anions (hereafter abbreviated as cubane-dc) are reported. The product is obtained by coprecipitation method when solutions of M(II) and M(III) salts react with an alkaline solution of the cubane-1, 4- dicarboxylic acid. At the first step, an experimental analysis concerning powder X-ray diffraction, FTIR spectroscopy, thermal gravimetric analysis (TGA), and SEM was performed for characterization of the LDH nanohybrid. Computational simulations were established to understand the structural and electronic properties of the cubane-dc-Zn_2Al-LDH system. Then, comparison of the experimental solid state UV absorbance and subsequently band gap energy with simulated optical property and band structure results, which involve DOS, molecular orbital, and band gap calculations, are reported.

2. Experimental

2.1. Materials

Cubane-1,4-dicarboxylic acid was prepared by the methods described in the literature.[27,28] All reagents were purchased from Merck chemical company and used without further purification. NO_3-Zn–Al-LDH was prepared according to the literature.[7]

2.2. Characterizations

Powder X-ray diffraction patterns (PXRD) of the samples were recorded by a Bruker AXS model D8 Advance diffract meter using Cu-K_α radiation (λ = 1.54 Å) at 40 kV, 35 mA with a Bragg angle ranging from 2 to 70° 2Θ. Fourier transform infrared spectra (FT-IR) were recorded in the range of 4000–400 cm^{-1} using the KBr pellet technique with a Perkin-Elmer spectrophotometer. TGA was carried out with a Mettler-Toledo TGA 851e apparatus at the heating rate of 10 $Kmin^{-1}$ in the nitrogen atmosphere. The scanning electron microscopy (SEM) was used to study morphology of the samples using ultrahigh resolution FESEM device, model ULTRA55, Carl Zeiss MST AG, Germany. Zn and Al contents of the samples were determined using inductively coupled plasma spectroscopy (Jobin Yvon JY24) after dissolving the samples in nitric acid. Elemental (C, H, and N) analyses were carried out on a Perkin-Elmer 240B analyzer. Diffuse reflectance spectrum (DRS) was recorded using the wavelength monitoring method by absorbance ranging from 200 nm to 1000 nm (Firmware Version: 061020 Software Version: LabPro Plus Build 410.1)

2.3. Syntheses of cubane-dc–Zn-Al-LDH

Cubane-dc–Zn-Al-LDH was prepared as previously described.[26] So, a solution containing the cubane-1,4-dicarboxylic acid (0.172 g, 0.001 mol) dissolved in NaOH (20 mL, 0.1 M) was slowly added to an aqueous mixed solution (20 mL) of $Zn(NO_3)_2{\cdot}6H_2O$ (0.5949 g, 0.002 mol) and $Al(NO_3)_3{\cdot}9H_2O$ (0.375 g, 0.001 mol) with vigorous stirring in the nitrogen atmosphere. The pH of the collection was adjusted to 8.3 by dropwise adding of NaOH or HCl. The system was heated to reflux at 55 °C for 72 h under nitrogen atmosphere. The product (cubane-dc-Zn_2Al-LDH) was centrifuged at the speed of 2000 rpm for 10 min and the solid was washed thoroughly with deionized water and finally dried at room temperature in vacuum. Anal. calculated for $[Zn_4Al_2(OH)_{12}](C_{10}H_6O_4){\cdot}3H_2O$: C, 15.72; H,

3.17; Zn, 34.24; Al, 7.06. Found: C, 15.3; H, 2.7; Zn, 34.0; Al, 6.6.

2.4. Molecular modelling

Complete simulations were carried out using the $Dmol_3$ and Discover modules in the Materials Studio Software Package.[29] This modules involve a range of fine-certified functions and force fields for quantum mechanics and molecular dynamics simulations, minimization, and analysis searches for periodic solids. In this research, a perfect Zn-Al-LDH layer model with hexagonal supercell was made. At first, DFT method was used to get the geometry optimization configuration for the cubane-dc anions. After determination of the atomic charges, this information was used in the molecular mechanic minimization by classical force fields and additional quantum mechanics computation. Fundamental works on the modeling for the first developed *CLAYFF* [30] force field (FF) that was particularly appropriate to deal with LDHs containing Si, Al, Mg, Ca, Fe, and Li , and this force field was more subsequently implemented and validated[31] with parameters for LDHs in which M(II) was Zn^{2+} cation.[32-37] A large number of force fields, such as Dreiding force field,[38] universal force field (UFF),[39] Compass,[40] and consistent force field (CFF),[41]have been developed for different material systems. As for LDH simulation, a modified Dreiding force field4 and *CLAYFF* force field [30,42] are mostly used. The former was explored by Newman et al. The latter (ClayFF) was originally designed by Cygan et al.[30] for modeling clay materials, which relies basically on van der Waals and the coordination configurations of central metal coulombic interactions instead of covalent bonds to maintain cations (either tetrahedral or octahedral). Such a nonbonded model can be directly inserted into other well-developed force fields and shows high computational efficiency.[43]

Therefore, the classical *Dreiding* force field was used for the cubane-dc-Zn_2Al-LDH system .[44-46]

The first step in arranging models of intercalates was the construction of the host positively charged Zn-Al-LDH layeres. The hydroxide layeres of $[Zn_4Al_2\ (OH)_{12}CO_3.3H_2O]$ were built using atomic coordinates from the previously reported crystal structure of the hydrotalcite. The host structure was made of three layers and it included a rhombohedral lattice with hexagonal unit cell parameters of a=b= 3.06616 A˚, c = 22.6164 A˚, α =β = 90◦, γ= 120◦ [47] and the space group of $R3^{-}m$. In order to study the mutual arrangement of the guests in the interlayer space, a P1 supercell with the dimensions of 6a×4a ×$3d_{exp}$ was developed where d_{exp} was obtained from the x-ray diffraction data of cubane-dc-Zn-Al-LDH. The interlamellar carbonate ions and water molecules were omitted, then a 3a × 2b × 1.8c supercell was developed with lattice parameters of 3a =9.19848 Å, 2b =6.13232 Å, and 1.80c =40.71 Å, where d_{exp} =13.57 Å. The ratio of Zn and Al atoms in the framework was 2:1, and the Zn and Al atoms were scattered arbitrarily in every layer. Every hydroxide layer had $2Al^{3+}$ and $4Zn^{2+}$ ions, with the latter arranged in a way that they were not placed in the adjacent octahedral. The cubane-dc anions were randomly located in the interlamellar area of the LDH to neutralize the positive charges for the hybrid system, and then to form a tilted bilayer arrangement. The molecules of water (4 molecules) were also randomly inserted into the interlamellar area. The atomic charges can be determined from the mulliken, APT, and ESP charges. In this work ESP method [48] was used for the calculation of atomic charges. Figure 1 shows ESP charges of the cubane-dc anion. $Dmol_3$ program at the GGA-PBE/DND level optimized the cubane-dc structure. The atomic charges are essential in explaining the cubane-dc structure and the QM study when cubane-dc anions positioned into the LDH layers.

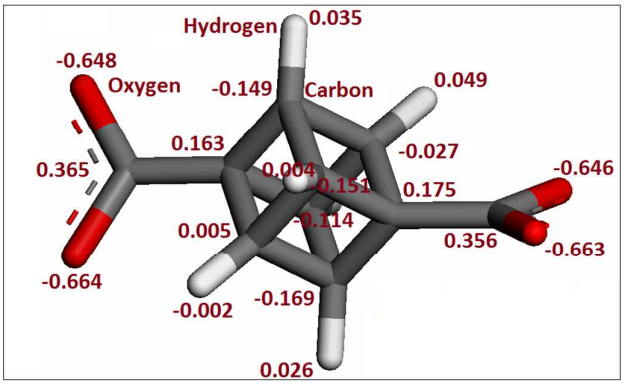

Fig. 1 ESP atomic charges of cubane-DC

Layer charges were initially calculated by the charge equilibration (QEq) method. Since the *Dreiding* force field is suitable for Zn-Al- LDH [49], the LDH part charges were improved with regard to the Dreiding force field, while the partial charge for Al was set to 1.319e or 1.412e, for Zn to 0.373e or 0.426e, for O to -0.438e or -0.552e, and for H to 0.226e or 0.341e.

The initial configuration was fully optimized by *Dreiding* force field. The electrostatic energy was found by the *Ewald* summation method [50] and the van der Waals energy was shown by the Lennard–Jones potential.[51] The total crystal energy minimization was conducted by a modified smart minimizer method according to the following approach: all the layers of the host were kept as firm units in the energy minimization period and the cell parameters c, a, and b were variable. This enabled optimization of the mutual arrangement of the host layers. All the atomic positions in the interlayer region were variable to [52] and then further optimization was implemented by the Perdew–Burke–Ernzerhof (PBE) generalized gradient approximation (GGA) with the double numerical basis sets plus polarization function (DNP). The core electrons of the metals were treated by the Electron (AE) method. SCF converged criterion was within 1.0×10^{-5} hartree/atom. The Brillouin zone was sampled by Γ(0, 0, 0) k-points (Gamma), and test calculations confirm that the increase of k-points does not influence the results. This results are in agreement with results reported by Yan et al for poly(p-phenylene)/layered double hydroxide [53,54] and bis(2-sulfona-tostyryl)biphenyl/layered double hydroxide.[55] All calculations were done with the periodic density functional theory (DFT) method using $Dmol_3$ [56,57] modules. Fig. 2 shows final optimized supercell of cubane-dc-Zn_2Al-LDH.

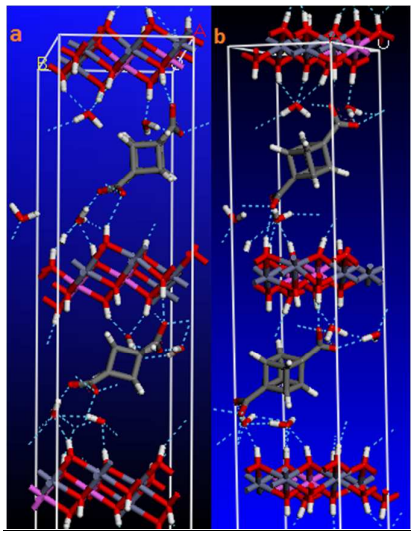

Fig. 2 Final optimized supercell of cubane-dc-Zn_2Al-LDH via quantum mechanics calculation in two sights (a and b)

3. Results and Discussion

3.1. XRD analyses

The XRD pattern of Zn-Al-NO_3-LDH and cuban-dc-Zn_2Al-LDH showed characteristic reflections related to the crystalline layered phase (Figure 3).[58,59] In the range of 2-70° for Zn_2Al-NO_3-LDH, the sharp and strong diffraction peaks at low 2θ values, shown in Fig. 3(a), demonstrate good crystallinity of the LDH nanoparticles.

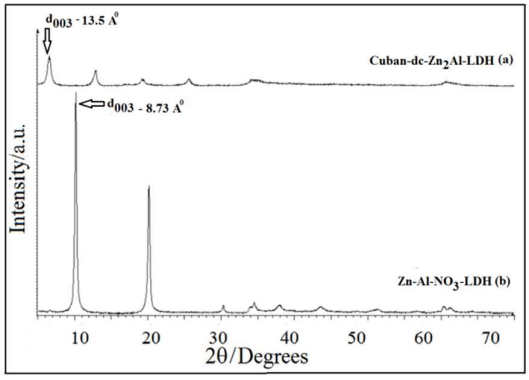

Fig. 3 PXRD patterns of Zn-al-NO_3-LDH and Zn-Al-LDH intercalated with cubane-DC- Zn-Al-LDH

Zn-Al-NO_3-LDH has d_{003} basal spacing of 8.73 Å. The basal spacing value of d_{003}, representing the summation of thickness of the brucite-like layer (0.48 nm)[60] and the gallery height, is a function of the number, size, and orientation of the intercalated anions.[61]

The XRD pattern of cuban-dc-Zn_2Al-LDH is shown in Figure 3(b). During the intercalation of the cubane-dc anions, the layers of LDH swell to host the anions and this expansion is reflected by the value of d_{003}. The value of d_{003} is 13.57 Å. This swelling of the layers is due to the intercalation of the cubane-dc anions and the basal spacing corresponding to the diffraction by planes (003) was much larger than that of LDH. Since the thickness of LDH layer is 4.8 Å and the longitudinal Van der Waals' radius of the cubane-dc anion is 7.14 Å (determined by the software ChemSketch), it was confirmed that cubane-dc anions were successfully intercalated in their anionic form, and that they were arranged as a monolayer within the interlayer.

3.2. FTIR Spectra

Cubane-dc-Zn_2Al-LDH was also confirmed by the FT-IR spectroscopy. The FT-IR spectra of the cubane-1, 4 dicarboxylic acid, Zn_2Al-NO_3-LDH, and cubane-dc-Zn-Al-LDH are shown in Figure 4(a)–(c).

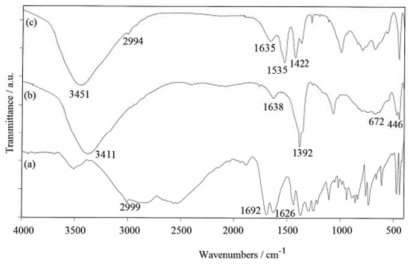

Fig. 4 FT-IR spectra of (a) cubane-1, 4 dicarboxylic acid, (b) Zn–Al–NO_3-LDH, and (c) cubane-DC-Zn_2Al-LDH

The spectrum for Zn–Al–NO_3-LDH is similar to that reported in the literature.[62,63] Absorption at 1392 cm^{-1} can be assigned to the ν_3 vibration of NO_3. A broad strong absorption band centred at 3411 cm^{-1} is ascribed to the stretching vibrations of hydroxyl groups and surface and interlayer water molecules, [64,65] which are found at a lower frequency in LDHs compared with the O–H stretching in free water at 3600 cm^{-1}.[66] This is attributed to the formation of hydrogen bands between the interlayer water molecules and the different guest anions as well as the hydroxide groups of the layers. A weaker band at 1638 cm^{-1} was due to the bending mode of the water molecules. The bands centred at 446 and 672 cm^{-1} are attributed to the al–O and Zn–O lattice vibrations.[62]

In case of the pure cubane -1, 4-dicarboxylic acid, strong absorption bands centred at 3416 cm^{-1} and 3500 cm^{-1} are attributed to the stretching vibrations of the OH groups. Furthermore, the absorption bands at 1692 and 1626 cm^{-1} are related to the C=O of the carboxylate groups. Absence of the NO_3 bands at 1392 cm^{-1} in the spectrum of LDH indicates that the preparation process was complete. The band at 1692 and 1626 cm^{-1} attributable to the COOH group disappears, while two bands at 1535 and 1422 cm^{-1} attributable to the anti-symmetric and symmetric stretching vibrations of $–COO^-$ appear and shift to lower wavenumbers, compared to free –COOH in cubane -1, 4 dicarboxylic acid. This indicates that the intercalation in the interlayer space involves hydrogen banding, besides the obvious electrostatic attraction between the electropositive cations in the layer and organic anions in the interlayer.[61,67,68]

3.3. Thermal analyses

Suitable tools for determining thermal stability of the material are thermogravimetric analyses (TGA).The thermal stability of the cubane -1,4-dicarboxylic acid and cubane-dc-Zn_2Al-LDH are investigated using TGA analysis. The TGA

curves are shown in figure 5(a) and pristine Zn-Al-LDH-NO3 is shown in figure 5(b). In case of the cubane-1,4-dicarboxylic acid there are two steps in the temperature range of 220–300 °C and 300-500 °C that are attributed to the decomposition of cubane-1,4-dicarboxylic acid. The mass loss value at 850 °C of the cubane -1, 4-dicarboxylic acid is 87.5%.

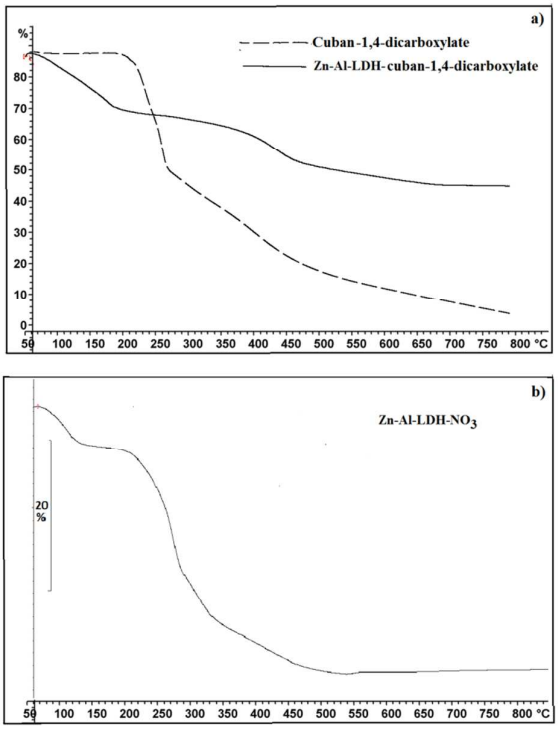

Fig. 5 TGA thermograms of (a) cubane-1,4dicarboxylic acid, and Zn-Al-LDH-cubane-dc, and (b) pristine Zn-Al-LDH-NO_3.

Cubane-dc-LDH shows major mass losses in three steps. The first mass loss observed in 50–200 °C corresponds to the loss of both adsorbed and interlayer water molecules. The second one in the range of 210–430 °C is attributable to the cubane-dc decomposition and dehydroxylation of the LDH layer. The third one in the temperature range of 430–600 °C is attributed to further dehydroxylation of the LDH layers. The mass loss value at 850 °C of cubane-DC -LDH is 46.1%. In case of the Zn-Al-LDH-NO_3 (Figure 5b)there are two steps in the temperature range of 160–250 °C and250-480 °C.The first mass loss corresponds to the loss of both adsorbed and interlayer water molecules.The second one in the range of 250–480 °C is attributedto the nitrate ions decomposition and dehydroxylation of the LDH layer.The mass loss value at 870 °C of the Zn-Al-LDH-NO_3 is 38.1%.

3.4. SEM

A scanning electron microscopy (SEM) image of the cubane-DC- LDH nanohybride is depicted in Fig. 6. The irregular sheet-like character of the cubane-dc-Zn_2Al-LDH nanohybride can be seen clearly in this figure. In fact cubane-dc-Zn_2Al-LDH is composed of aggregates of irregular sheet-like nanoparticles with sheet thicknesses in the range of 20–40 nm. The broadening of the XRD pattern of cubane-DC-Zn_2Al-LDH (Fig. 3) is due to the nanosize of the particles.

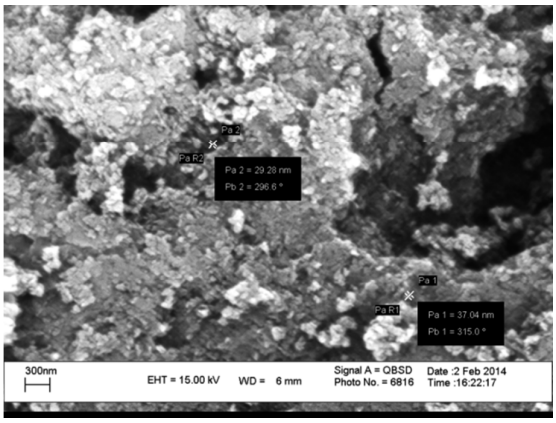

Fig. 6 SEM image of Cubane-DC- Zn_2Al-LDH

3.5. Results of the molecular modelling and simulation

3.5.1. Comparison of experimental and calculated XRD

The positioning of cubane-dc anions within the interlayer space of Zn_2Al-LDH depends on the space available to the guest anions in the interlayer region. On the basis of the d_{003} value of cubane-dc-Zn_2Al-LDH (measured by x-ray diffraction), the space accessible to the cubane-dc anions in the interlayer space is 8.6 Å, which can be calculated approximately by subtracting the layer thickness of 4.8 Å from the interlayer spacing (13.57 Å). According to the longitudinal Van der Waals' radius of the cubane-dc anion (7.20 Å), sufficient vacant space is available for the guest anions. On the other hand the orientation of the guest anions depends on the interactions of the guest anions with LDH layers, interlayer water molecules, and also guest-guest anions.

Experimental XRD results combined with molecular simulations can determine possible orientations of the cubane-dc guest anions in the interlayer space. The water content of the interlayer space and the position of the interlayer water molecules, and also the orientation of the guest anions strongly influenced the x-ray diffraction patterns. Using molecular modelling, initial molecular minimization, and quantum mechanics calculations, the water molecules and guest anions arranged inside the interlayer so that the calculated XRD pattern agrees with the measured one. Figure 7 shows the calculated QM and experimental XRD pattern for cubane-dc-Zn_2Al-LDH. According to the calculated XRD pattern, calculated $d_{003,}$ d_{006}, and d_{009} is 13.55 Å, 7.05 Å , and 4.48 Å respectively which is in good agreement with the experimental basal spacing (d_{003} = 13.57 Å). As can be seen from Fig. 7, the slightly higher value of the experimental d_{006} spacing compared to that of the calculated d_{006} may be related to the effect of crystal size on peak broadening as well as to the high disorder of the guests in the structural model, which is not taken into account in the software. [5] Besides, XRD anisotropic peak

broadening is another factor that can deform the lattice and cause peak shift because of non-spherical and nano-crystallite structure of cubane-dc-Zn_2Al-LDH, residual stress, crystal defects, and equipment reasons. These are fairly typical in the solid solutions.

We previously reported [26] (Fig. S1) the experimental XRD pattern of cubane-dc-Mg_2Al-LDH, which is the Mg analogue of cubane-dc-Zn_2Al-LDH. The comparison of XRD pattern of cubane-dc-Mg_2Al-LDH and cubane-dc-Zn_2Al-LDH (this work) with the related calculated XRD patterns showed that the intensity of the (003) and (006) peaks in cubane-dc-Zn_2Al-LDH are in good agreement with its calculated pattern. While this comparison in cubane-dc-Mg_2Al-LDH (previous work) shows that the intensity of the mentioned peaks was inverted. Based on the literature, the roughness of the surface of the experimental sample (cubane-dc-Mg_2Al-LDH), which is not considered in the software, is responsible for the inversion of the intensity of the (003) and (006) peaks. But in cubane-dc-Zn_2Al-LDH, as can be seen in Fig. 7, good agreement between experimental diffraction pattern and the calculated XRD pattern reveals that the surface of cubane-dc- Zn-Al-LDH is regular.

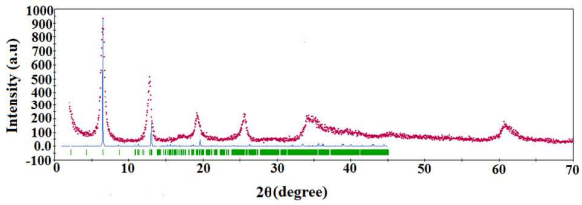

Fig. 7 The calculated (solid line) and experimental (dashed line) x-ray diffraction patterns of cubane-dc- Zn-Al-LDH

3.5.2. Population Analysis

The population analysis which involves bond length investigation, the mulliken atomic charges, and mulliken bonding population was performed by density functional theory (DFT) calculations.

Bond lengths of Al–O and Zn–O, after geometric optimization of cubane-dc-Zn_2Al-LDH, which is calculated for the isolated layer without interlayer anions, are 1.833 Å and 1.939 Å respectively. After insertion of cubane-dc as interlayer anions, noticeable increase of Al–O and Zn–O bond lengths were observed, and the distances of al–O and Zn–O were also observed to be elongated to 1.927 Å and 2.224 Å respectively. Based on literature, the average distances of Al–O and Zn–O in Zaccagnaite-3R (natural hydrotalcites of $[Zn_4Al_2(OH)_{12}]CO_3.3H_2O$) [47] were 2.030 Å. These indicated that the metal cations of the layer were exhaustively attracted by the interlayer anions. Therefore, there were complex electrostatic interactions between the positive layers and the interlayer anions.

The mulliken atomic charges for cubane-dc-Zn_2Al-LDH were calculated. For the isolated layer, the mulliken atomic charges of Al and Zn cations were 1.749e and 1.138e, and for the O atoms of the layer were -1.015e. After importing interlayer anions, the mulliken atomic charges of Al and Zn cations became 0.883e and 0.795e and for O atoms of the layer it became -0.829e. This indicated that the charges have transferred from the guest anion to the metals of the host layer.

Mulliken bonding population of Al–O, Zn–O, and O–H of the isolated layers were 0.7281e, 0.2618e, and 0.5319e. Furthermore, the layer was looked upon as a whole to investigate the super-molecular interactions by **geometry optimization** between the host layer and the guest anions. After inserting the interlayerd cubane-dc anions, the Al–O, Zn–O, and O-H mulliken bonding population decreased to reach 0.2926e, 0.1076e, and 0.4590e respectively. It suggested that there were super-molecular interactions between the host layer and the guest anions, which seems to be the competitive effect of the electrostatic interactions and hydrogen bonding network.[8] These indicated that not only the electrovalent bands, but also the covalent bands existed between the metals and the hydroxyl groups in the LDHs-layer. The decrease of ***Mulliken bonding population*** of Al–O, Zn–O, and O–H after the insertion of interlayerd cubane-dc anions was compared to other LDHs with small anions e.g. $Mg_6Al_2(OH)_{16}X_2$(X=Halogenes) [8],and showed that changes in bond length and charge population in cubane-dc-Zn_2Al-LDH are greater than those of LDHs with small intercalated anions, such as halogens and main metals of layers without d orbitals.

3.5.3. Band Structure

For further investigation of the structural characteristics of the prepared LDH, the UV–vis-DRS spectra were recorded in the 200–800nm region. The DRS spectrum of cubane-dc-Zn_2Al-LDH is illustrated in Fig. 8a. The cubane-dc-Zn_2Al-LDH sample shows one absorption edge around 320 nm, that should be attributed to the absorption edge of Eg_1 , and another peak, Eg_2, that emerged at 377 nm .The optical band gap energies (Eg) of cubane-DC-Zn_2Al-LDH was determined by UV-vis- DRS, and the obtained DRS results are reported as the Kubelka–Munk function[69,70](Fig. 8b, inset).

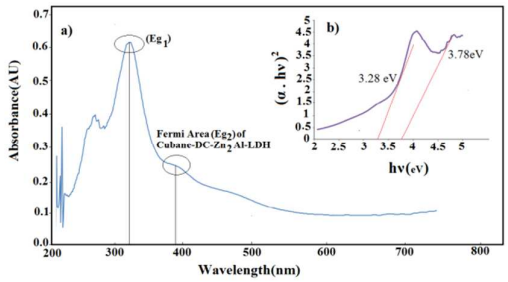

Fig 8. a) Diffuse reflectance spectroscopy(DRS)-UV-visible absorption spectrum , and b) Kubelka–Munk transformed reflectance spectrum for cubane-dc-Zn_2Al-LDH

Through measuring UV–vis-DRS, the band gap energy (Eg) of cubane-dc-Zn_2Al-LDH was determined. Determination of E_g for the sample was done using the Kubelka–Munk (K–M) Eq. (1):

$$\alpha = \frac{(1-R)^2}{2R} \qquad (1)$$

where R is the reflectance and α is the Kubelka–Munk function. The experimental values of the two band gap

energies calculated for cubane-DC-Zn_2Al-LDH are: Eg1=3.76 eV and Eg_2=3.28 eV, which are indicated in Fig. 8.

The band gap of the cubane-dc-Zn_2Al-LDH system was calculated by the GGA- PBE function (Figure S2) for better understanding of the electronic band structure and for receiving electronic structure information for the effect of the metal elements in the LDH layers and the main atoms of the interlayer organic anions on the UV absorption capacity. Reciprocal points in the Brillouin Zone(BZ) for calculation were set to G(0,0,0), F(0,1/2,0), Z (0,0,1/2), and Q (0, 1/2,1/2). Also we tested 2×1×1 *k*-points for band structure calculation and this different *k*-point caused same result (3.26 eV) for band gap. So test calculations reveal that the increase of *k*-points does not affect the results.

Fig S1 indicates that the energy gap between conduction band (CB) and valance band (VB) at G point (0,0,0) in the first Brillouin Zone is 3.26 eV which are in good agreement with the gap band energy attributed to the experimental DRS (diffuse reflectance spectroscopy) results.

Absorbance spectrum results from experimental DRS spectrum and subsequently experimental band gap energies in Fig. 8(a, b) indicate that cubane-dc-Zn_2Al-LDH has UV absorbance value around 320 nm (3.76 ev) and 377 nm (3.28 eV) that were attributed to Eg_1 and Eg_2 (band gap energies) of cubane-dc-Zn_2Al-LDH respectively. These results show that the cubane-dc anions with carboxylic head groups when intercalated in Zn-Al-LDH have caused red shift and also decrease of band gap energy in comparison with electronic structure of Zn–Al–NO_3-LDH [23] as the LDHs contain small anions. So cubane-dc-Zn-Al-LDH can have gap energy near that of the luxurious photocatalytic material such as TiO_2 (3.23 eV), ZnO(3.21 eV), ZnS(3.60 eV), and α-Fe_2O_3(3.1 eV).[71,72] The calculated optical absorption spectrum of cubane-dc-Zn_2Al-LDH (Fig. S3), using quantum mechanics calculations, is in good agreement with the experimental diffuse reflectance spectroscopy.

3.5.4. DOS and PDOS

For the purpose of understanding the electronic structure of cubane-dc-Zn_2Al-LDH, after the band structure analysis, the densities of states (DOS) as well as the partial densities of states (PDOS) were investigated by density functional theory (DFT) calculations for the supercell model of cubane-dc-Zn_2Al-LDH. The total density of states (DOS) and the partial densities of states (PDOS) were performed to understand the rearrangement of the electron density in the atoms which participate in energy transfer system of cubane-dc-Zn_2Al-LDH.

The DOS and PDOS of cubane-dc-Zn_2Al-LDH and interlayer anions are shown in Fig. 9 and Fig. 10. It can be observed from Fig. 9 and Fig. 10 that for the cubane-dc-Zn_2Al-LDH system, the top of the valence band (TVB) is mainly located on the conjugated 3d orbitals of Zn atoms in the layers and partly 2p orbitals of O atoms of the cubane-dc anions, and the bottom of the conducting band (BCB) is mainly located on the conjugated 2p orbitals of C atoms of the cubane-dc anions and partially on the 3p orbital of Al atoms of the layeres. Around the Fermi energy (-0.1607 Ha=-4.375 eV), PDOS mainly consists of the 3d electrons of Zn atoms in the layer. The gap of cubane-dc-Zn_2Al-LDH was determined by the energy difference between the LUMOs (lowest unoccupied), 2p orbitals of C atoms, HOMOs (highest occupied), and 3d orbitals of Zn atoms. [20] Electrons will transit to a higher energy level when the gap of the energy levels decreases, and the chemical stability of the cubane-dc-Zn_2Al-LDH system gets worse. According to Fig. 9 and Fig. 10, in the energy range of -0.21 Ha to -0.16 Ha of DOS, 3d orbitals of Zn atoms and 2p orbitals of O atoms in the layers afforded the major contributions, and 2p orbitals of C and O atoms of cubane-dc anions, 3s orbitals of Al, 2p orbitals of O atoms of water molecules, and 2p orbitals of O atoms of the layers afforded partial contributions. In the energy range of -0.15 Ha to -0.25 Ha, 3d orbitals of Zn atoms, 2p orbitals of C and O atoms of cubane-dc molecules, 2p orbitals of O atoms of the layer, and in the energy range of -0.65 Ha to -0.78Ha of DOS, 3d orbitals of Zn atoms, 3s orbitals of Al atoms, 2s orbitals of C and O atoms of cubane-DC molecules, 2s orbitals of the O layer, 2s orbitals of O atoms of waters, and 1s orbitals of H atoms of water molecules and of the layers afforded major contributions, and in this energy range, 3s orbitals of Al atoms and 2p orbitals of water molecules had partial contributions.[8]

The investigation of the electronic properties was an essential step for understanding the chemical activities of LDHs. The influence of the different atomic orbitals on the formation of the chemical bonds has been quantitatively analyzed. The quasi atomic calculations delivered initial electron distributions of Zn as $3d^{10}$ $4s^2$, Al as $3s^2$ $3p^1$, O as $2s^2$ $2p^4$,H as $1s^2$,and C as $2s^2$ $2p^2$,but the calculated true electron distribution of O is $2s^{0.938}$ $2p^{2.615}$ $3d^{0.013}$, Zn is $4s^{0.191}$ $3d^{4.996}4p^{0.203}$, Al is $3s^{0.173}$ $3p^{0.238}$ $3d^{0.111}$, and H is $1s^{0.239}$ of the LDH layers; O is $2s^{0.912}$ $2p^{2.424}$ $3d^{0.022}$, C is $2s^{0.534}$ $2p^{1.063}$ $3d^{0.122}$, and H is $1s^{0.390}$ of the cubane-dc anions; O is $2s^{0.944}$ $2p^{2.575}$ $3d^{0.018}$ and H is $1s^{0.231}$ of the water molecules. Most of the electrons on s orbitals of Zn (4s) and Al (3s) were to a certain extent delocalized. But the electrons on the p orbitals of Al (3p) and d orbit of Zn (3d) were localized by the oxygen atoms of the layers. On the other hand, most of the electrons on s orbitals of O(2s) and C(2s) of the cubane-dc anions were localized by the interlayer hydrogen atoms of the water molecules .In contrast, the electrons on p orbitals of O (2p) and C (2p) of the cubane-dc anions were to a small extent delocalized. It can be concluded that electrostatic interactions and hydrogen bonding existed between the host layer and the guest anions. These indicated that both electrovalent and hydrogen bands existed among the atoms of the layer and the intercalated cubane-dc anions and the water molecules. And the p orbital of the metal cations and s orbital of the guest anions provided major contributions to the covalent parts of the system, while the s orbital of the metal cations and p orbital of the guest anions provided major contributions to the electrovalent parts.[8]

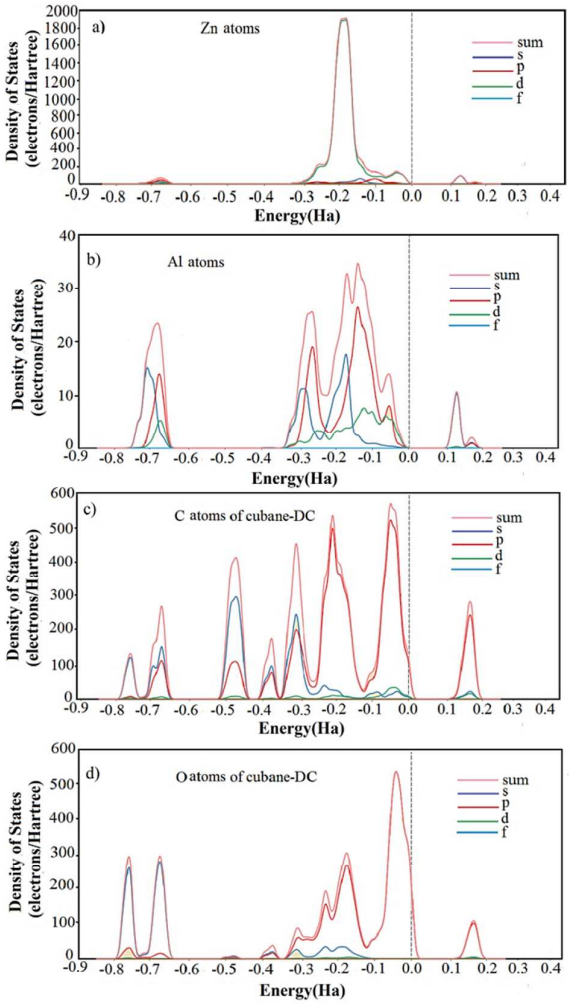

Fig. 9 The DOS (density of state) and PDOS (partial density of state) of Zn and Al atoms of the LDH layer and O, C atoms of the cubane-dicarboxylate anions in cubane-dc-Zn_2Al-LDH (a-d).

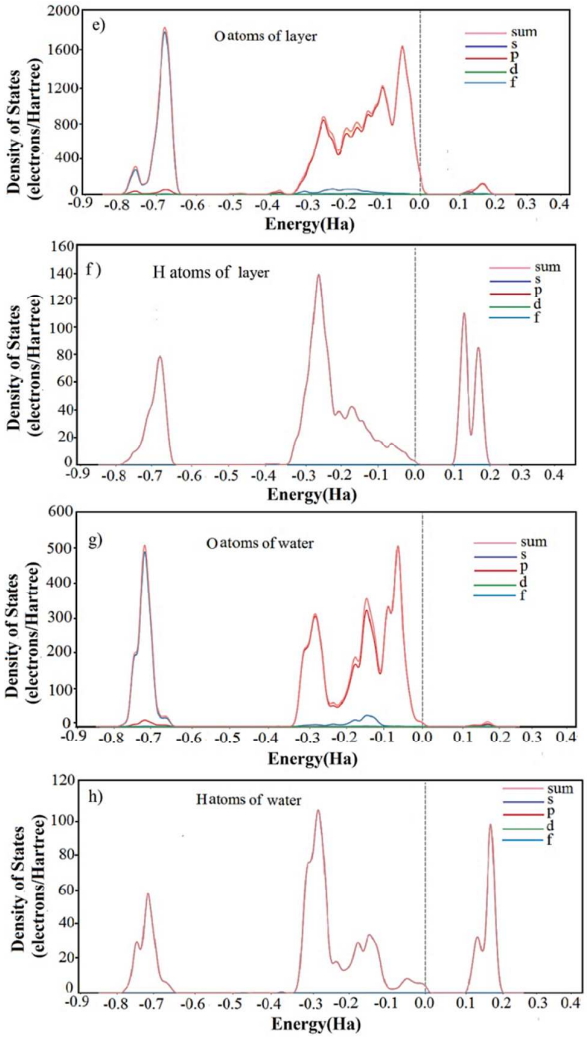

Fig. 10 The DOS (density of state) and PDOS (partial density of state) of O, and H atoms of the LDH layer and O, H atoms of the water molecules in cubane-dc-Zn_2Al-LDH(e-h).

It can be observed from Fig. 11 that HOMOs are mainly distributed on the O atoms of the carboxylate group and the LUMOs, comprised of two degeneration orbitals, are mainly located on the C atoms of the cubane-dicarboxylate anions .This result is comparable with Fig 9 that was resulted from PDOS analysis of C and O atoms of the cubane-dc anions .The results demonstrate that hydrogen atoms of the cubane dicarboxylate anion does not influence the excitation and emission processes of the cubane dicarboxylate anion in the cubane-dc-Zn_2Al-LDH system.[20] Based on the intercalated anion, total electronic densities of states (TDOS) and partial electronic densities of states (PDOS) analysis (Fig. 9) reveal that 2p orbitals of the oxygen atoms and 2p orbitals of the carbon atoms contribute to TDOS below and above HOMO and LUMO, respectively.(Fig. 11)

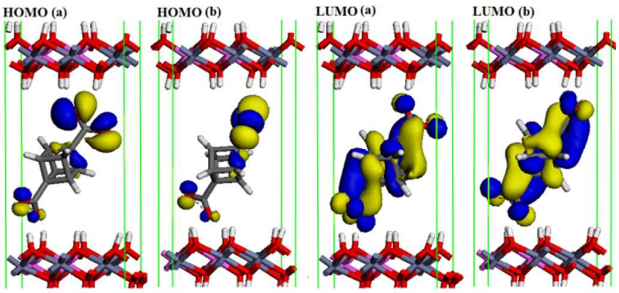

Fig. 11. The typical HOMO and LUMO profiles calculated by PBE for the cubane-DC Molecule

Conclusions

The synthesis and characterization of the Zn–Al hydrotalcite intercalated with the cubane-dc anions are reported in the present research. Successful intercalation of the cubane-1,4-dicarboxylate anions into the interlayer space of Zn_2Al-LDH was confirmed by powder X-ray diffraction, FTIR spectroscopy, thermal gravimetric analysis (TGA), and scanning electron microscopy (SEM). During the intercalation of the cubane-dc anions, the layers of LDH swell to host the anions, and this expansion is reflected by the value of d_{003}. A quantum mechanics simulation was used to investigate the band structural and optical properties of the cubane-dc-Zn_2Al-LDH system. These results are in good agreement with experimented crystal structural (XRD), band–structural (gap energy), and optical (DRS spectrum) properties. The DOS calculation with the DFT method and the molecular orbital models in cubane-dc-Zn_2Al-LDH confirm calculated band structure results and the optical property of the simulation part. These results show that the Zn-Al-LDH containing cubane-dc anions as large intercalated anions have band gap energy of 3.28 eV which is lower than the Zn–Al–NO_3-LDH band gap energy (3.8 eV) with small intercalated anion.

Acknowledgements

We are grateful for the support from Azarbaijan Shahid Madani University. We also thank the research laboratory of Dr M. Mahkam (Azarbaijan Shahid Madani University) for preparation of cubane-1,4-dicarboxylic acid.

Notes and references

1 V. Rives, *Layered Double Hydroxides: Present and Future*, Nova Sci Pub Inc , 2001.
2 M.R. Perez, I. Pavlovic, C. Barriga, J. Cornejo, M.C. Hermosin, and M.A. Ulibarri, *Appl. Clay Sci*., 2006, **32**, 245–251.
3 F. Cavani, F. Trifiro, and A.Vaccari, *Catal.Today*., 1991, **11,** 173–301.
4 G. Wang, D. Rao, K. Li, and Y. Lin, *Eng. Chem. Res*., 2014, **53**, 4165–4172.
5 P. Kovar, K. Melanova, V. Zima, L. Benes, and P. C. Apkova, *J. Colloid Interface Sci*., 2008, **319**,19-24.
6 H. Zhang, Z. P. Xu, G. Q. Lu, and S. C. Smith, *Phys. Chem*. C, 2009, **113**, 559-566.
7 A. A. A. Ahmed, Z.A. Talib, M.Z. Hussein, and A. Zakaria, *J. Solid State Chemistry.*, 2012, **191**, 271- 278.
8 Q. Xu, Z.M. Ni, and J.H. Mao, *J. Molecular Structure*., 2009, **915**,122–131.
9 D. Yan, Y. Zhao, M. Wei, R. Liang, J.Lu, D.G. Evans, and X. Duan, *RSC Advances.,* 2013, **3**,4303-4310.
10 D. Yan, R. Gao, M. Wei, S. Li, J. Lu, D. G. Evans, and X. Duan, *J. Mater. Chem. C*, 2013, **1**, 997-1004
11 D. Yan, J. Lu, J. Ma, M. Wei, D.G. Evans, and X. Duan , *AIChE J*., 2011, **57,** 1926-1935.
12 D. Yan ,J. Lu, J. Ma, M. Wei, S. Li, D. G. Evans, and X. Duan, *Phys.Chem*. C, 2011, **115**, 7939-7945
13 A. G. Kalinichev, R.J. Kirkpatrick and R.T. Cygan, *American Mineralogist*., 2000, **85**,1046-1052.
14 H. C. Greenwell, W. Jones, P.V. Coveney, and S.J. Stackhouse, *J. Mater. Chem.,* 2006, **16**, 708-723.
15 R.T. Cygan, *Reviews in Mineralogy and Geochemistry*., 2001, **42**,1-35.
16 N. Kim, Y. Kim, T.T. Tsotsis, and M. Sahimi, *J. Chem. Phys.,* 2005,**122**, 214713-12.
17 N. Kim, A. Harale, T. T. Tsotsis, and M. Sahimi, *J. Chem. Phys.,* 2007, **127**, 224701-12.
18 D.G. Costa, A.B. Rocha, R. Diniz, W. F. Souza, S. S. X. Chiaro, and A. A. Leitao, *J. Phys. Chem. C,* 2010, **114**,14133–14140.
19 K. Owski, W. Macyk, A. Drzewiecka-Matuszek, M. Brindell, and G. Stochel, *Chem. Rev*., 2005, **105**, 2647-2694.
20 D. Yan, S. Qin, L. Chen, J. Lu, J. Ma, M. Wei, D.G. Evans, and X. Duana, *Chem. Commun*., 2010,**46**, 8654-8656.
21 Y. Zhao, B. Li, Q. Wang, W. Gao, C. J. Wang, M. Wei, D. G. Evans, X. Duan, and D. O'Hare, Chem. Sci., 2014, **5**, 951-958.
22 R.T. Cygan, J.A. Greathouse, H. Heinz, and A.G. Kalinichev , *J. Mater Chem.,* 2009, **19,** 2470–2481.
23 H. Chai, X. Xu, Y. Lin, D.G. Evans, and D. Li, *Polym. Degrad.Stab*., 2009 , **94** ,744–749.
24 A.A.A. Ahmed, Z.A. Talib, M.Z. Hussein, *Appl. Clay Sci*., 2012, **56**,68–76.
25 K. Jayasuriya, S. Iyer, *struct.chem*., 1990, **1**,165-170.
26 Z. Rezvani, F. Arjomandi Rad and F. Khodam, *Dalton Trans*., 2015, **44**, 988-996.
27 K. Hassenruck, J.G. Radziszewski, V. Balaji, G.S. Murthy, A.J. Mckinley, D.E. David, V. N. Lynch, H. D. Martin, and J. Michl, *J. Am. Chem. Soc*., 1990, **112**, 873.
28 N. B. Chapman, J. M. Key, and K. J. Toyne, *J. Org. Chem*.,1970, **35**, 3860-3867.
29 *Discover, User Guide*, Accelrys, Molecular Simulations Inc, San Diego, USA ,1996.
30 R.T. Cygan, J.J. Liang, A.G. Kalinichev, *J. Phys. Chem. B,* 2004,**108,** 1255–1266.
31 G. M. Lombardo, G.C. Pappalardo, F. Punzo, F. Costantino, U. Costantino, and M. Sisani, *Eur. J. Inorg. Chem.* 2005, **24**, 5026–5034.
32 G.M.Lombardo,G.C.Pappalardo,F.Stantino , U.Ostantino, and M. Sisani, *Chem. Mater*. 2008,**20**, 5585-5592.
33 M. Mezei , S. Swaminathan , and D.L. Beveridge, *Journal of Physical Chemistry B*., 2008, **112**, 7856−7864.
34 M.A.Thyveetil , P.V. Coveney , J.L. Suter , and H.C. Greenwell,*Chem.Mater.*, 2007, ***19,*** 5510–5523.
35 H. Li, J. Ma, D.G. Evans, T. Zhou, F. Li, and X. Duan, *Chem. Mater*.2006, **18,** 4405−4414.

36 P. P. Kumar , A.G. Kalinichev , and R.J. Kirkpatrick**,** *Journal of Physical Chemistry C*, 2007, **111,** 13517-13523.
37 A.G. Kalinichev, P.P. Kumar, and R.J. Kirkpatrick, *Philosophical Magazine*, 2010, 90, 2475–2488.
38 S.L. Mayo , B.D. Olafson , and W.A. Goddard,*J. Phys. Chem.* 1990,**94,** 8897-8909.
39 A.K. Rappe , C. J. Casewit , K. S. Colwell , W. A. Goddard III, and W. M. Skiff*J. Am. Chem. Soc.* 1992, **114**, 10024-10035.
40 H. Sun, *J. Phys. Chem*. B 1998, **102,** 7338-7364.
41 S. Lifson, and A. Warshel, *J. Chem. Phys*. 1968, **49,** 5116-5129.
42 J. Pisson, J. P. Morel, N. Morel-Desrosiers, C. Taviot-Gue´ho, and P. Malfreyt,*J. Phys. Chem. B*, 2008, **112**, 7856−7864.
43 S.T. Zhang, H.Yan, M. Wei, D.G. Evans, and X. Duan, *J. Phys. Chem. C*, 2012, **116**, 3421−3431.
44 J. L. Zhang, M. Zhang, J. J.Wan, and W. Li, *J. Phys.Chem.B*, 2008, **112**, 36-43.
45 V. Varshney, S. S. Patnaik, A.K. Roy, and B.L. Farmer, *J. Phys.Chem.C*, 2010, **114**, 16223-16228.
46 G.Raffaini, and F. Ganazzoli, *J. Phys. Chem. B*, 2010, **114** ,7133-7139.
47 R.P. lozano, C. Rossi, A.L. iglesia, and E. matesanz, *American Mineralogist*., 2012, **97***,* 513–523.
48 W.D. Cornell, P. Cieplak, C.I. Bayly, I.R. Gould, K.M. Merz, D.M. Ferguson, D.C. Spellmeyer, T. Fox, J.W. Caldwell, and P.A. Kollman, *J. Am.Chem. Soc*.,1995, **117**, 5179–5197.
49 S.P. Newman,T.D. Cristina, P.V. Coveney, and W. Jones, *Langmuir*., 2002,18,2933
50 N. Karasawa, and W.A. Goddard, *J. Phys. Chem*., 1989,**93** ,7320-7327.
51 J. E. Lennard-Jones, *Proc.R. Soc. Lond*. A, 1925, **109** , 584-597.
52 K. Lv, H. Kang, H. Zhang, and S. Yuan, *Colloids.Surf*. A, 2012, **402**,108-116.
53 D. Yan, J. Lu, M.Wei, J. Han, J. Ma, F. Li, D.G. Evans, and X. Duan, *Angew. Chem. Int. Ed*. 2009, **48,** 3073 –3076
54 D.Yan,J. Lu , J. Ma , M. Wei ,X. Wang ,D.G, Evans ,and X.Duan, *Langmuir.* 2010, 18; 26(10):7007-7014.
55 D. Yan, J. Lu, J. Ma, M. Wei1, D. G. Evans, and X. Duan, *Angew. Chem. Int. Ed.* 2011, **50,** 720-723.
56 B. Delley, *J. Chem. Phys*., 1990, **92**, 508-517.
57 B. Delley, J. *Chem. Phys*., 2000, **113**, 7756-7764.
58A.N. Ay, B. Z. Karan, and A. Temel, *Microporous Mesoporous Mater*., 2007, **98**, 1-3.
59 P. Kustrowski, D.Sulkowska, L.Chmielarz, A. Rafalska-Lasocha, B. Dudek, and R. Dziembaj, *Microporous Mesoporous Mater*., 2005, **78**, 11-22.
60 C. Li, G. Wang, D. G. Evans, and X. Duan, *J. Solid State Chem*., 2004, **177**, 4569-4575.
61 J.T. Klopprogge, L. Hickey, and J. L. Frost, *Appl. Clay Sci*.,2001, **18**, 37-49.
62 M. Wei, X. Xu, J. He, Q. Yuan, G. Rao, D. G. Evans, M. Pu, and L. Yang, *J. Phys. Chem. Solids.,* 2006, **67**, 1469-1476.
63 F. Cavani, F. Trifiro, and A. Vaccari, *Catal.Today.*, 1991, **11**,173-301.
64 K. Nakamoto, *Infrared and Raman Spectra of Inorganic and Coordination Compounds,* Wiley, New York, 5th edn, 1997.
65 S. J. Santosa, E. S. Kunarti, and E. Karmanto, *Appl. Surf. Sci*., 2008, **254**, 7612-7617.
66 H. Gunzler, and H. U. Gremlich, *IR Spectroscopy:An Introduction*, Wiley-VCH, Weinheim, 2002.
67 H. Zhang, K. Zou, S. Guo, and X. Duan, *J. Solid State Chem*.,2006, **179**, 1792-1801.
68 X. Duan, and D. G. Evans, *Structure and Banding*., 2006,**119**, 89-119.
69 H.M. ali, M.M. Abou-Mesalam, and M.M. El-Shorbagy, *J. Phys. Chem. Solids*., 2010, **71**, 51-55.
70 K.H. Reddy, S. Martha, and K.M. Parida, *Inorganic Chemistry*., 2013,**52** , 6390-6401.
71 M.R. Hoffmann, S.T. Martin, W.Y. Choi, and D.W. Bahnemann, *Chem. Rev*.,1995,**95**, 69–96.
72 A.V. Emeline, G.V. Kataeva, V.K. Ryabchuk, and N. Serpone, *J. Phys. Chem*. B, 1999, **103**, 9190–9199.

